Appropriate Data for Validation of Large Eddy Simulation of Flows with Evaporating Drops

S. Radhakrishnan[1] and J. Bellan[1,2*]
Jet Propulsion Laboratory[1]
California Institute of Technology
Pasadena CA 91109-8099 USA
Mechanical Engineering Department[2]
California Institute of Technology
Pasadena CA 91125 USA

Abstract

A methodology is developed to identify experimental results appropriate for validating Large Eddy Simulation (LES) for spray computations. Validation is defined as a process through which the fidelity of a mathematical model (and numerical scheme) to represent a process is ascertained. The purpose of validation is to discriminate correct from incorrect physics so as to identify a model which can be used with confidence for situations in which experimental data is not available. It is proposed that validation should be user driven in that objectives should be first defined, and then the required experimental data for validation can be identified in a rigorous manner for those objectives. A database of Direct Numerical Simulation (DNS) is considered as an ideal experimental database in which all information is available. LES errors are defined with respect to the filtered-and-coarsened DNS (FC-DNS) which is the ideal, unachievable LES. Objectives are defined, and LES is compared to the FC-DNS for these objectives. Through error computations based on physical quantities one can identify those physical quantities which can discriminate among various LES models. Physical quantities which cannot discriminate among various LES models are considered unsuited to be appropriate data for model validation since they fail in their primary goal of distinguishing between correct and incorrect physics. Results are presented for several objectives, testing the proposed concept and methodology.

Introduction

Large Eddy Simulation (LES) is a promising methodology for the computationally efficient prediction of turbulent flows because the calculation aims at the accurate solution of the large, energy containing scales which are of primary engineering interest and relies on models for the more universal small scales, thereby minimizing computational costs. The LES equations are obtained through filtering of the Navier-Stokes equations which are the exact continuum-flow equations describing the physical situation. The effect of the filtered small-scale motion on resolved large scale motion appears as Subgrid-Scale (SGS) terms in the LES equation and it depends on the detailed - i.e. all-scales - flow field which is unavailable; instead, these terms must be modeled. This modeling is typically done through representing the small-scale terms as functions of the only solved-for and known entity: the large scale solution. Of course, the accurate modeling of the filtered small-scale effects is essential for the accurate prediction of the large scales.

The LES methodology originated in the context of atmospheric-science flows, that is, for incompressible, single species turbulent flows. As LES showed promise, this methodology has also been extended to atmospheric-pressure compressible single-phase flows, to describing the gas phase of atmospheric-pressure condensed-phase volumetrically-dilute particle-laden flows, and to high-pressure flows; also, binary-species flows were considered in all these situations. These extensions involve additional SGS flux terms (heat and species) for compressible flows, added filtered source terms (FST) for two-phase flows that account for the interaction between the two phases in the flow [1, 2], and extra subgrid terms for high-pressure turbulence accounting for the strong non-linearity of the real-gas equation of state [3].

The accuracy of the flow field predicted by LES depends on both the SGS model as well as the numerical procedure (discretization scheme, grid, etc.) used. The numerical procedure cannot be independently considered from the SGS model since in the typical LES, the accuracy of the SGS model depends on the smallest resolved scales (SRS) which are influenced by the truncation and aliasing errors; also, the SRS sizes are determined by the LES grid. These observations have already appeared in the literature [4, 5, 6] (e.g. the observation [6] that LES is usually executed as an "incomplete" model) but its implications have not been fully studied. Since the LES prediction depends both on the SGS model and the numerics, it is recognized that experimental validation is essential to give confidence in the predictive capability

*Josette Bellan

of LES. But what is the nature of the experimental data necessary to validate LES? In a utilitarian way, this depends on how much detail is necessary for the application at hand. From the general viewpoint of determining whether a model appropriately describes the physics, this is yet a question to be addressed, and of course, the answer depends on the specific physics. A rigorous methodology to address the relationship among the three entities of SGS models, discretization scheme and numerical resolution, and experiments has not yet been proposed, yet developing such fundamental understanding is of paramount importance in creating predictive computational capabilities.

The purpose of model validation is determining whether the LES model is correct because it is only under these circumstances that it can be utilized for the purpose of predictive simulations treating situations in which experimental data is not available. We propose that if the type of experimental data used for model validation cannot discriminate among SGS models embodying different physics, it is not appropriate for LES model validation because it cannot distinguish between correct and incorrect physics. The goal is here to identify the type of experimental data (e.g. gas or drop velocity measurements, drop size measurements, etc.) which discriminates among different SGS models. Of course, the type of experimental data depends on the objectives of the particular application for which the simulation will be used. Because we wish to choose measurements from an ideal experimental database, defined as one in which all measurements are available, we consider the DNS database as such an ideal, surrogate, experimental database. However, for model validation, LES cannot be compared to DNS because the resolution is not at the same scale. Rather, the LES comparison should be made with the filtered-and-coarsened DNS (FC-DNS): filtered to remove the small scales and coarsened to retain only the LES nodes. The FC-DNS is the ideal, usually unachievable, LES solution which is the template for our investigation.

Definition of objectives

Spray evaporation is the first step in combustion processes relying on fuel injection and atomization. From the combustion perspective, a model which computes spray evaporation should accurately predict quantities that are essential in reactive processes which include the velocity field, root mean square (r.m.s.) of the velocity components, temperature distribution, vapor mass fraction, the species flux directionality, mean and r.m.s. of the droplet velocities, etc. These are a few examples of objectives which are the focus of a designer. In experiments, due to the limitation of measuring devices, often only few of the above objectives are measured. When validation of the models is done with the limited measurements available from the experiments, often many models predict some of these measured quantities accurately even when other quantities predicted by these models differ. Our goal is to identify objectives that are of interest for designing spray devices and for which the prediction varies with models. These are the quantities that will be pertinent in identifying correct from incorrect physics.

Description of the governing equations and the database

The DNS and LES governing equations have been described in detail and listed elsewhere [7] and thus will only be summarized here. The equations describe the motion of a collection of drops in a flow under the assumption that the drop volumetric loading is small, thus allowing the point-source approximation for the drops in the flow. There is a two-way interaction between the flow field represented in DNS by the vector of gas-phase conservative variables $\phi = \{\rho,\ \rho u_i,\ \rho e_t,\ \rho Y_V\}$ (where ρ is the density, u_i is the velocity in the x_i coordinate direction, e_t is the total energy and Y_V is the vapor (subscript V) mass fraction (the carrier gas, subscript C, mass fraction is Y_C; $Y_C + Y_V = 1$)) and the drop field defined by $Z = \{X_i, v_i, T_d, m_d\}$ with position X_i, velocity v_i, temperature T_d, and mass m_d. The gas phase is followed in an Eulerian frame and the drop field is followed in a Lagrangian frame. The flow-field governing equations are the continuity, momentum, species and total energy equations complemented by the perfect gas equation of state. The drop-field equations are written for each physical drop and are for the trajectory, mass, momentum and energy equations with the assumptions that drops are spherical and have constant liquid density, ρ_L. The drop influence on the gas is manifested through source terms in all flow field conservation equations accounting for addition of mass to the gas phase through evaporation, for drag on each drop and for heat transfer from the gas to the drops as well as for energy addition by the evaporation-created vapor which enters the gas with the drop velocity. The effect of the gas on the drops is manifested by an evaporation-originated sink term in the drop-mass equation, by a drag term in the drop momentum equation and by two terms in every drop energy equation, portraying drop heating and the thermodynamics of evaporation through the latent heat.

The LES equations are obtained by filtering the Navier-Stokes equations using a top-hat filter $\overline{\Delta}$, and are solved for the filtered flow field $\bar{\phi}$ and a computational drop field $\bar{Z}$ is obtained by dividing the physical number of drops N_d by a factor N_R; thus, each of the N_{cd} computational drops represents $N_R \equiv N_d/N_{cd}$ physical drops. Each of the N_{cd} drops follows the Lagrangian drop field evolution equations. The LES set of equations is not mathematically

complete in that it requires two types of models to enable conducting simulations: SGS-flux models representing the filtered small scales, and FST models representing the influence of the drops on the flow field when the drop field is reduced and the gas-phase variables must be computed at the N_{cd} drop location from a flow field which is calculated on a much coarser grid than that of DNS.

The physical configuration is that of a temporal mixing layer having streamwise (x_1), cross-stream (x_2), and spanwise (x_3) coordinates with dimensions $L_1 \times L_2 \times L_3$ of 0.2m×0.44m×0.12m. Periodic boundary conditions are used in the x_1 and x_3 directions, and adiabatic slip wall conditions [8] are employed for the x_2 boundaries. The domain has a cross-stream height larger by a factor of two from the previous DNS [1] in order to reduce the effect of reflected waves from the adiabatic slip boundaries. Drops reaching the slip walls are assumed to stick to the wall, but are otherwise transported according to the drop equations. Initially, the gas phase consists only of the carrier gas (air with no vapor); the initial mean streamwise velocity $\langle u_1 \rangle$, where $\langle\rangle$ denotes $(x_1,\, x_3)$ homogeneous plane averaging, has an error-function profile. To promote layer growth, the layer is initially perturbed so as to induce roll-up and pairing. The perturbations specify spanwise and streamwise vorticity fluctuations [9] and the evolution of the layer comprises two pairings of the four initial spanwise vortices to form a single vortex. A total number of 15,113,680 drops, corresponding to a mass loading ratio (ratio of liquid mass to the lower-stream carrier-gas mass) of 0.5, are initially distributed randomly throughout the $x_2 < 0$ domain; the initial velocity of each drop is the same as that of the gas phase at its location. Because the domain is larger by a factor of 2 from that used in [1], so is the number of drops in the computation. The drops are at a temperature of 345 K which is lower than their boiling point (447.7 K) and also lower than the temperature of air (375 K). The drop size variation is specified through the initial Stokes number, $St = \tau_d \Delta U_0/\delta_{\omega,0}$, given by a normal distribution with mean 3 and standard deviation of 0.5, where $\tau_d = \rho_L d^2/(18\mu)$, d is the drop diameter, μ is the gas viscosity, $\Delta U_0 = 2U_0$ is the velocity difference across the layer, $U_0 = M_{c,0} a_{C,0}$, is calculated from a specified value of convective Mach number $M_{c,0}$ based on the carrier gas initial speed of sound $a_{C,0}$, and $\delta_{\omega,0} = \delta_\omega\,(0)$ is the initial vorticity thickness where $\delta_\omega\,(t) = \Delta U_0/\left(\partial \langle u_1 \rangle/\partial x_2\right)_{\max}$.

The DNS were performed using a fourth-order explicit Runge-Kutta scheme for temporal integration, an eighth-order central finite differencing scheme for spatial discretization and with a tenth-order filter to remove aliasing errors [10]; this filter introduces a small amount of dissipation that serves only to stabilize the computations for long-time integrations and does not affect the physics of the problem. A fourth-order Lagrange interpolation procedure is used to obtain gas-phase variable values at the drop locations [11]. The same numerical scheme is used in LES to ensure that when LES results are compared to the FC-DNS they truly represent the effect of modeling rather than combined modeling and numerics. The LES are initiated at $t = 0$ with the FC-DNS initial condition and the N_{cd} subset of the DNS drop field.

Results

The FC-DNS is obtained from DNS computations utilizing the same grid spacing, initial Reynolds number $\mathrm{Re}_0 = \rho_0 \Delta U_0 \delta_{\omega,0}/\mu$, where ρ_0 is the initial gas density as the calculations of [1] and [2]. The grid has (288×640×176) nodes and the grid spacing is $\Delta x_{DNS,i}$ in each i direction. The initial value of the Reynolds number, Re_0, based on the vorticity thickness is 600 and $M_{c,0} = 0.35$. The DNS was performed up to a non-dimensional time, $t^* \equiv t\Delta U_0/\delta_{\omega,0} = 200$, which is longer than that of the DNS of [1] so that here a higher Re value is achieved. At $t^* = 200$, $\mathrm{Re}_m = \mathrm{Re}_0(\delta_m/\delta_{\omega,0}) = 1765$ in the DNS, where the momentum thickness δ_m has been defined in [1]. All the presented statistics (e.g. mean) are obtained by averaging along $(x_1,\, x_3)$ homogeneous planes.

LES were performed with constant-coefficient Smagorinsky model (SMC), the dynamic Smagorinsky model (SMD), the constant coefficient Gradient model (GRC), the dynamic Gradient model (GRD) and the Scale-Similarity model (SSC). For SMC and GRC, we used the DNS calibrated coefficient values listed in [1], which were obtained at $t^*_{tr} = 100$ where tr stands for the transitional time identified as that where the one-dimensional energy spectra are smooth except for the peak at the forcing frequency. For all LES, the grid $\Delta x_{LES,i} = 4\Delta x_{DNS,i}$ for all i. The top-hat filter is utilized, and $\overline{\Delta} = \max_{i=1,2,3}(\Delta x_{LES,i})$. In all LES, $N_R = 16$. Figure 1 shows the time history of $\delta_m/\delta_{\omega,0}$ which measures the layer growth; of the x_2-integrated non-dimensionalized gas kinetic energy E_{kG}/E_0 where

$$E_{kG} = \left(\int_{-L_2}^{L_2} (\frac{1}{2}\rho \left(\sum_{i=1}^{3} < u_i^2 >\right) dx_2\right), \tag{1}$$

$$E_0 = \left[\int_{-L_2}^{L_2} (C_v T_0 + \frac{1}{2}\rho \left(\sum_{i=1}^{3} < u_{i,0}^2 >\right) dx_2\right] + \sum_{\alpha=1}^{N_{d,0}} m_{d\alpha} \left[C_{pd} T_{d,0} + \frac{1}{2}\left(\sum_{i=1}^{3} v_{i,0}^2\right)\right]_\alpha, \tag{2}$$

C_v is the heat capacity at constant volume, T is the gas temperature of which the reference is at 0 degrees Kelvin, subscript d identifies drop quantities, and subscript 0 identifies the initial condition; of the x_2-integrated enstrophy $\int_{-L_2}^{L_2} < \omega_i\omega_i > dx_2$ where $\boldsymbol{\omega}$ is the vorticity vector; and of the x_2-integrated non-dimensionalized gas internal energy E_{iG}/E_0 where $E_{iG} = \left(\int_{-L_2}^{L_2} C_v T dx_2\right)$. The SMC model predicts a much lower $\delta_m/\delta_{\omega,0}$ growth (figure 1a) during the transitional stage than the FC-DNS which is improved by the SMD model whereas the SSC model consistently under-predicts the $\delta_m/\delta_{\omega,0}$ growth. Both GRC and GRD show good prediction up to t^*_{tr} after which they underpredict $\delta_m/\delta_{\omega,0}$. While comparison of $\delta_m/\delta_{\omega,0}$ with the FC-DNS can identify the deficiencies of the SSC model, the quantity $\delta_m/\delta_{\omega,0}$ cannot discriminate between the two versions of the Gradient and of the Smagorinsky models, making it unreliable for experimental validation. A similar conclusion is reached when we compare the prediction of E_{kG}/E_0 by all the other models with FC-DNS (figure 1b). In contrast to these two quantities, $\int_{-L_2}^{L_2} \omega_i\omega_i \, dx_2$, seen in figure 1c, can differentiate among the performance of various models: the SSC model consistently underpredicts it while the Gradient model shows initially a good match and underpredicts this quantity during the transition stage, with reasonable agreement during the turbulent stage. Both versions of the Smagorinsky model underpredict enstrophy up to the transition stage and they show overprediction during the turbulent stage. Comparison of various model performance shows that the Gradient model performs better than all the other models, and enstrophy has the ability to discriminate between various models. Figure 1d shows the growth of E_{iG}/E_0 from the enhancement due to dissipation (of mean kinetic energy, of turbulent kinetic energy, and of scalar and temperature gradients) and to the energy supply from the vapor entering the gas, and from the reduction due to heat transfer from gas to the drops. For LES, the deviation of E_{iG}/E_0 from the FC-DNS results is a total measure of the error from the combined SGS-flux and FST models; however, all differences are relatively small. To explore the influence of the FST model, the fraction of drops $N_{cd}/N_{cd,0}$ and the ratio $\left\{d^2\right\} = \left(\sum_{\alpha=1}^{N_{cd}} d_\alpha^2\right)/N_{cd}$ to the square of the average diameter at $t^* = 0$ are plotted. The information in figure 2a shows that more drops have vaporized in SSC, GRC and GRD LES than in SMC and SMD LES runs, which means that approximately more energy has been extracted from the flow in the SMC and SMD LES than in the SSC, GRC and GRD LES but also that more vapor mass entered the gas at the evaporation temperature. However, in all cases, the difference from the FC-DNS is small, making $N_{cd}/N_{cd,0}$ unsuited as an experimental measurement for model validation. Figure 2b shows that $\left\{d^2\right\} / \left\{d_0^2\right\}$ is slightly overpredicted by Gradient and SSC model runs and underpredicted by Smagorinsky model runs compared to FC-DNS even though all LES computations are initiated with the same N_{cd}; however, all LES closely agree with the FC-DNS, making $\left\{d^2\right\} / \left\{d_0^2\right\}$ also unsuited for model validation.

Figure 3a shows the (x_1, x_3) Favre averaged u_1 prediction by each model at $t^* = 200$. The SSC model predicts a much less developed velocity profile whereas all other models predict the Favre averaged velocity reasonably well. However, overall, the difference between models and FC-DNS is rather small, thus making the Favre averaged u_1 unsuited for model validation. For reactive flows, the accurate prediction of the vapor mass fraction and turbulent vapor flux is essential as the latter plays an important role in large scale species mixing. Figure 3b shows that all models predict the vapor mass fraction reasonably well except for SMC which overpredicts it near the top stream. Figure 3c depicts the resolved turbulent vapor mass flux $\left\langle \rho u_2'' Y_v'' \right\rangle$ where $u_2'' = (u_2 - < \rho u_2 > / < \rho >)$ and $Y_v'' = (Y_v - < \rho Y_v > / < \rho >)$. All models show an underprediction of the peak value while the SMC underpredicts it near the center line of the mixing layer by as much as 50%. M_d, which denotes the mass of all drops in a volume extending over the (x_1, x_3) plane and half-grid spacing along x_2 on either sides of the computational nodes, is illustrated in figure 3d . Compared to the FC-DNS, SMC predicts an inaccurate drop mass x_2-distribution, with an excess near the top part of the layer. The differences in turbulent vapor flux and the drop mass x_2-distribution will clearly result in inaccurate prediction of the reaction rates in reactive flows. For this reason, the utilization of the SMC model is not recommended. Thus, the turbulent vapor flux and the drop mass x_2-distribution have the potential to discriminate between various LES models.

Summary and Conclusions

Several SGS-flux models were assessed by comparing them to the FC-DNS for the purpose of identifying quantities which can discriminate among model predictions. Several such global quantities were considered, such as the momentum thickness growth, the kinetic energy, the enstrophy, the internal energy, the drop number and the drop-ensemble-average diameter evolution. Also investigated were the profiles of the Favre averaged streamwise velocity, the vapor mass fraction, the turbulent vapor flux and the drop-ensemble-average mass spatial x_2-distribution. Among global quantities, only the enstrophy could be used to discriminate the various model performance. Among spatial x_2-

distributions, only the turbulent vapor flux and the drop mass were found appropriate quantities for model validation. The Favre-averaged streamwise velocity, much used for model validation, was found unsuited for this purpose.

Acknowledgments

This study was conducted at the Jet Propulsion Laboratory (JPL), California Institute of Technology (Caltech) and sponsored by NASA jointly under the Fundamental Aeronautics Program with Drs. Dan Bulzan and Nan-Suey Liu serving as program monitors, and under the LASER program in the ESMD/Advanced Capabilities Division.

References

1. Okong'o, N. and Bellan, J., J. Fluid Mech. 499:1-47 (2004).
2. Leboissetier, A., Okong'o, N. and Bellan, J., J. Fluid Mech. 523:37-78 (2005).
3. Selle, L. C., Okong'o, N. A., Bellan, J. and Harstad, K. G., J. Fluid Mech. 593:57-91 (2007).
4. Vreman, B., Geurts, B. and Kuerten, H., Int. J. Num. Meth. Fluids 22:297-311 (1996).
5. Kravchenko, A. G. and Moin, P., J. Comp. Phys. 131:310-322 (1997).
6. Pope, S. B., New Journal of Physics 6:35-59 (2004).
7. Okong'o, N., Leboissetier, A. and Bellan, J., Physics of Fluids 20(10):103305 (1-16) (2008).
8. Poinsot, T.J. and Lele, S.K., J. Comp. Phys. 101, 104-129 (1992).
9. Moser, R.D. and Rogers, M.M., Phys. Fluids A 3(5):1128-1134 (1991).
10. Kennedy, C.A. and Carpenter, M.H., Appl. Num. Math. 14:397-433 (1994).
11. Miller, R.S. and Bellan, J., J. Fluid Mech. 384:293-338 (1999).

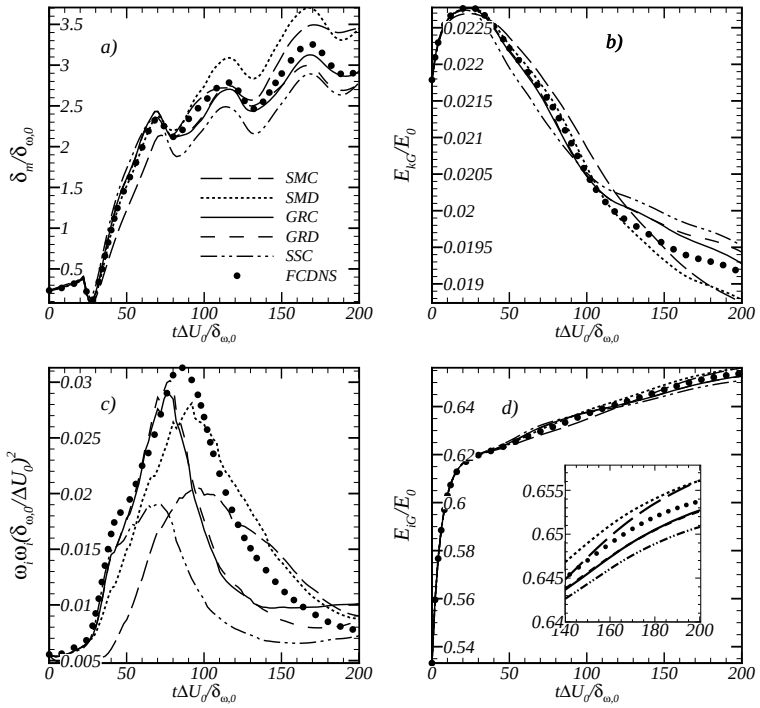

Figure 1. Temporal evolution of global quantities for FC-DNS and LES using various SGS-flux models for the same FST model with $N_R = 16$.

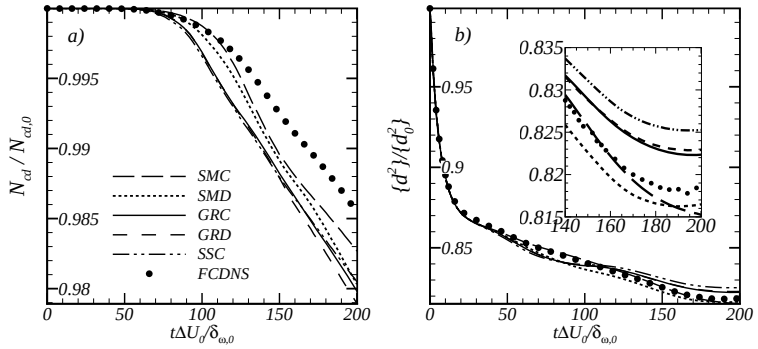

Figure 2. Temporal evolution of drop characteristics: a) non-dimensional drop number and b) ensemble-averaged non-dimensional drop diameter square.

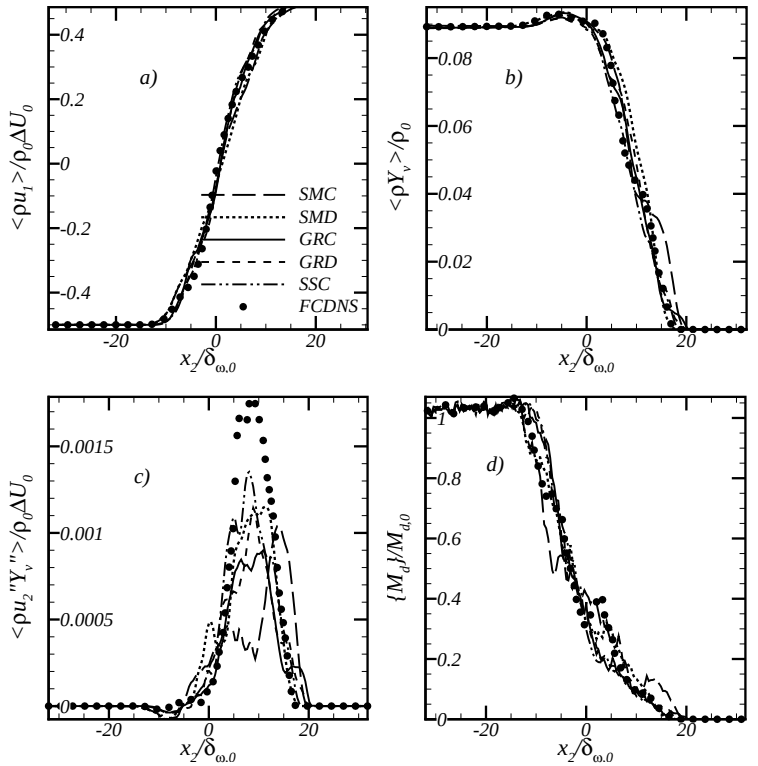

Figure 3. Cross-stream profiles at $t^* = 200$: (a) Favre-averaged streamwise velocity, (b) Favre-averaged vapor mass fraction, (c) resolved turbulent vapor flux and (d) fraction of remaining liquid drops.